Environ Sci Pollut Res (2015) 22:6864–6876
DOI 10.1007/s11356-014-3911-7

RESEARCH ARTICLE

PM_{10} concentration in urban atmosphere around the eastern Tien Shan, Central Asia during 2007–2013

Shengjie Wang · Mingjun Zhang · María Cruz Minguillón · Xiaoyu Zhang · Fang Feng · Xue Qiu

Received: 30 June 2014 / Accepted: 24 November 2014 / Published online: 4 December 2014

Abstract Based on the daily records from 16 cities around the eastern Tien Shan (Tianshan Mountains), central Asia from 2007 to 2013, the spatial pattern and seasonal/interannual variation of urban particulate matter up to 10 μm in size (PM_{10}) concentrations and influencing factors were analyzed. Annual mean PM_{10} concentrations (±standard deviation) in most cities on the northern slope mainly range from 55±28 μg/m^3 to 92±75 μg/m^3, and those on the southern slope range between 96±65 and 195±144 μg/m^3. PM_{10} concentrations are maxima in winter on the northern slope, while they maximize in springtime on the southern slope. There is an increasing trend in annual mean concentrations during the period 2007–2013, which is not statistically significant at the 0.05 level. Urban PM_{10} concentration in the study region is jointly influenced by anthropogenic emission and regional natural processes, especially dust events and precipitation. The northern slope usually has heavy anthropogenic air pollution (mostly in winter) and relatively rich precipitation especially in summer, and the southern slope always suffers more frequent dust events (mostly in spring) and less precipitation. Modeled back-trajectory indicated that the Taklimakan desert source can greatly increase the PM_{10} concentration on the southern slope, and the mountain ranges may hinder the transport of dust to the northern slope.

Keywords Particulate matter · Central Asia · Dust sources · Tien Shan

Introduction

Arid and semiarid land in central Asia is the main dust source in the Northern Hemisphere, and the regional aeolian dust may greatly influence eastern Asia and even North America (Zhang et al. 2003; Wang et al. 2008, 2011; Han et al. 2008; Liu et al. 2009; Maher et al. 2010; Ku and Park 2013; Groll et al. 2013; Dong et al. 2014). The Tien Shan (also known as Tianshan Mountains) is the main mountain range in central Asia, and many residents live at the narrow oasis belts of Tien Shan Corridor between the high mountains and low-lying deserts. Continuous monitoring of airborne particulate matter at these oases in the Tien Shan Corridor is necessary for air quality assessment and forecast as well as global change research (Yabuki et al. 2005; Li et al. 2008, 2011; Zhao et al. 2011; Chen et al. 2013).

Along the oases in the Tien Shan Corridor, the existing studies about urban particulate matter up to 10 μm in size (PM_{10}) monitoring mainly focused on Urumqi, the provincial capital city of Xinjiang Uygur Autonomous Region, northwest China (Feng et al. 2005; Li et al. 2008; Ma et al. 2010; Mamtimin and Meixner 2011). Research using a chemical mass balance receptor model (Feng et al. 2005) indicates that the major sources of PM_{10} in Urumqi include suspended dusts (30 %), coal combustion (28 %), and cement dusts (11 %). The mixing of the transported dust aerosol and the local anthropogenic emission was considered as the important

Responsible editor: Gerhard Lammel

Electronic supplementary material The online version of this article (doi:10.1007/s11356-014-3911-7) contains supplementary material, which is available to authorized users.

S. Wang · M. Zhang (✉) · X. Qiu
College of Geography and Environmental Science, Northwest Normal University, Lanzhou, China
e-mail: mjzhang2004@163.com

M. C. Minguillón
Institute of Environmental Assessment and Water Research (IDAEA), Spanish Council for Scientific Research (CSIC), Barcelona, Spain

X. Zhang · F. Feng
Cold and Arid Regions Environmental and Engineering Research Institute, Chinese Academy of Sciences, Lanzhou, China

factor causing the heavy atmospheric pollution in Urumqi (Li et al. 2008; Han et al. 2013). The variation of atmospheric pollution in Urumqi during the 2000s is greatly related with the growth of motor vehicles (Mamtimin and Meixner 2011; Wei 2011; Zheng 2014). The spatial pattern of PM_{10} concentration in Urumqi was also investigated, and the seasonality of particulate matters can be seen for each site (Ma et al. 2010; Wei 2012). Because of the extremely heavy pollution in the city of Urumqi, the high particulate matter loading in Urumqi cannot well represent the regional feature for the entire Tien Shan Corridor, and additional sites are necessary to assess the PM_{10} spatial-temporal variability for this region. In the past decade, more automatic monitoring network has been established by environmental authorities (Gu and Guo 2010; Guo et al. 2014). However, to the authors' knowledge, there are no systematic studies on other cities along the oasis belts.

In this paper, the aforementioned research gap is addressed, based on daily PM_{10} concentrations from 2007 to 2013 in 16 cities around the eastern Tien Shan. In addition, the anthropogenic emission and natural process (especially dust events and precipitation) influencing the urban PM_{10} distribution and variability are discussed.

Methodology

Study area

Many modern cities lie at the oasis belts on the northern and southern slopes of the eastern Tien Shan, between the high mountains and low-lying desert basins. In this study, 16 cities around the eastern Tien Shan were selected (Fig. 1 and Table S1 in the supplementary material), hosting a total urban population of approximately 7.7 million inhabitants. Among these cities, 10 cities are located on the northern slope of the main ridge of the eastern Tien Shan, and 6 cities lie on the southern slope. Urumqi is the provincial capital city of Xinjiang, China, and has the largest urban population and built-up area across the Tien Shan Corridor. In Xinjiang, there are only two observation sites (Urumqi and Karamay) belonging to the national network operated by the Ministry of Environmental Protection (MEP) of China, and the PM_{10} spatial-temporal variability for this region is still unclear in previous national-wide reports (e.g., Qu et al. 2010).

PM_{10} concentration

The daily PM_{10} concentrations during 2007–2013 were derived from the daily air pollution index (API) provided by the Xinjiang Department of Environmental Protection and the MEP of China. The original measurements and index calculation for each city followed the same national standards issued by MEP. The API is a semiquantitative measure for uniformly reporting daily air quality for each city, and the daily concentrations of the pollutants are converted into a dimensionless number from 0 to 500. The daily API is defined as the highest index among the individual indices of three prominent pollutants (PM_{10}, SO_2, and NO_2). Individual indices are calculated by linear interpolation of the observed concentration between the grading limits for each air quality level (see Table 1).

When PM_{10} is reported as a prominent pollutant, PM_{10} concentration can be derived from API by using the following equation:

$$c = \frac{I - I_{\mathrm{low}}}{I_{\mathrm{high}} - I_{\mathrm{low}}} \times \left(c_{\mathrm{high}} - c_{\mathrm{low}}\right) + c_{\mathrm{low}} \qquad (1)$$

where c is the PM_{10} concentration, I is the daily API, I_{low} and I_{high} are the API grading limits that are lower and larger than I, respectively, and c_{high} and c_{low} are the PM_{10} concentrations corresponding to I_{high} and I_{low} in Table 1, respectively. This method has been widely used in previous studies (e.g., Gong et al. 2007; Choi et al. 2008; Qu et al. 2010). The quality control method for the original daily API data consists of as follows: (i) excluding days with daily API ≤0 or API >500, (ii) excluding days labeled as equipment malfunction or power failure, and (iii) when two or more different API values exist on the same day, the later-uploaded record is used.

When the API <50 (i.e., air quality level I, PM_{10} concentration <50 μg/m^3, SO_2 concentration <50 μg/m^3, and NO_2 concentration <80 μg/m^3; see Table 1), no prominent pollutant is reported. This happened for 20.5 % (7564 records) of the total data (Table 2). For these data, PM_{10} was assumed as the prominent pollutant, and PM_{10} concentrations were calculated by using Eq. (1), given that the API in the study region generally reflected the PM_{10} loadings, as explained below. PM_{10} was the prominent pollutant for 98.8 % of the data with API >50, whereas SO_2 and NO_2 were only reported as prominent pollutants about 1 % of the time. Considering the cities separately, PM_{10} was the prominent pollutant between 98.5 and 100 % of the time, except for Urumqi (86.7 %). In this study, a total of 36,933 records of daily API were acquired. Subsequently, 36,572 daily PM_{10} concentrations were derived, corresponding to days when PM_{10} was the prominent pollutant or when no prominent pollutant was reported.

It should be noted that for the days with API=500 when PM_{10} is the prominent pollutant, the PM_{10} concentration usually exceeds 600 μg/m^3, the upper level for the air quality level V. For all the 36,933 API records in this study, only 371 records (1.0 %) equaled to 500. During these 371 days, the prominent pollutant was always PM_{10}. Such high concentrations were found in 11 cities, and only 4 cities had more than 20 days with API=500 during these 7 years, which were Turpan (47 days), Aksu (67 days), Artux (79 days), and Kashi (120 days). Hence, in the present study, when API=500, the daily PM_{10} concentration

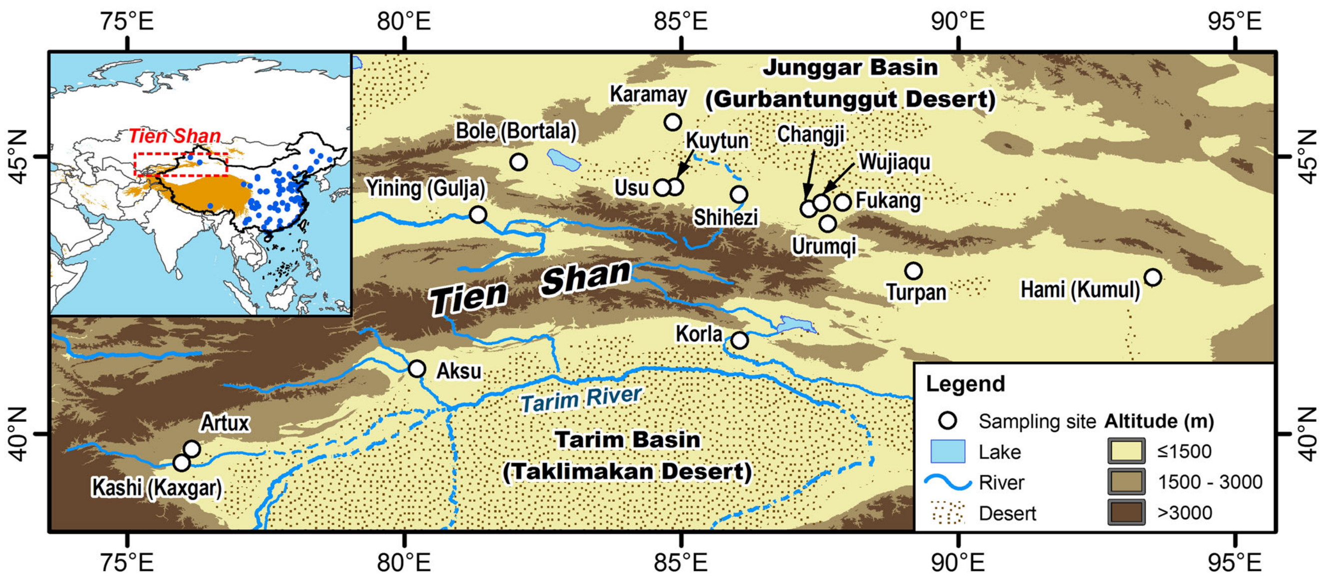

Fig. 1 Sampling sites over the eastern Tien Shan, central Asia. Locations of deserts are modified from Wang et al. (2005b). *Yellow shade* and *blue points* in the small map indicate altitude >2500 m above sea level and the existing stations in the national PM_{10} observation network settled by the Ministry of Environmental Protection of China (see Qu et al. 2010), respectively

was calculated as 600 μg/m^3, considering that the uncertainty introduced by this approximation should be quite limited.

In order to assess the reliability of API-derived PM_{10} concentration in this study, observed annual PM_{10} concentrations for each city published in the Xinjiang Statistical Yearbook (Statistics Bureau of Xinjiang Uygur Autonomous Region 2008, 2009, 2010, 2011, 2012, 2013) were collected. The measurement methods of PM_{10} concentration are described by the State Environmental Protection Administration of China (2003) and the Ministry of Environmental Protection of China (2011). As shown in Fig. 2, the annual average PM_{10} concentrations were calculated for each city. The API-derived concentrations correlate well with the yearbook-based averages (R^2=0.93, N=92), with a slope close to unity. The comparison between API-based and measured particulate matter concentrations in previous studies (e.g., Qu et al. 2010) also confirmed that this calculation method is acceptable in other regions of China.

Meteorology and others

Observed daily and monthly precipitation during 2007–2013 was provided by the National Meteorological Information Center (NMIC), China Meteorological Administration (CMA) (http://cdc.cma.gov.cn). Quality controls of meteorological data were employed, and the dataset was corrected when necessary (Li and Xiong 2004; Wang 2004). The weather records of dust events (such as dust storm, blowing dust, and floating dust events) were also acquired from NMIC (Wang et al. 2005a).

The Hybrid Single Particle Lagrangian Integrated Trajectory (HYSPLIT) model (Draxler and Hess 1998) version 4 and Real-time Environmental Applications and Display System (READY), developed by the NOAA's Air Resources Laboratory (http://www.arl.noaa.gov), were used to investigate the air mass origin reaching the study area and seasonality of atmospheric conditions. Two sets of gridded meteorological data were applied, including as follows: (i) National Centers for Environmental Prediction/ National Center for Atmospheric Research (NCEP/NCAR) Reanalysis data (2.5°×2.5°, six hourly), in modeling the 3-day back-trajectories to the given stations around the eastern Tien Shan, and (ii) NCEP Global Data Assimilation System (GDAS) archive data (1°×1°, three hourly), in calculating the daily/monthly boundary layer depth and atmospheric stability.

Table 1 Relationship between individual air pollution index (API) and corresponding concentration limits of pollutant

Air quality level	I	II	III	IV	V
API	0<API≤50	50<API≤100	100<API≤200	200<API≤300	300<API≤500
PM_{10} concentration (μg/m^3)	0<c≤50	50<c≤150	150<c≤350	350<c≤420	420<c≤600
SO_2 concentration (μg/m^3)	0<c≤50	50<c≤150	150<c≤800	800<c≤1600	1600<c≤2620
NO_2 concentration (μg/m^3)	0<c≤80	80<c≤120	120<c≤280	280<c≤565	565<c≤940

Table 2 Days with API>50 (in %) during 2007–2013 and days as prominent pollutant (in %) for PM_{10}, SO_2, and NO_2, for each city around the eastern Tien Shan

City		Days as prominent pollutant (%), from those with API >50			Days with API >50 (%)				
		PM_{10}	SO_2	NO_2	Annual	Spring	Summer	Autumn	Winter
Northern slope	Yining	99.2	0.3	0.5	92.0	88.9	90.3	92.3	96.4
	Bole	98.5	1.5	0.0	43.8	46.5	10.6	42.7	70.9
	Usu	99.6	0.1	0.3	68.4	64.7	47.0	73.3	86.1
	Karamay	99.8	0.2	0.0	66.3	64.1	52.6	73.6	75.0
	Kuytun	100.0	0.0	0.0	64.9	60.2	44.7	67.5	84.7
	Shihezi	98.5	1.4	0.1	67.2	61.0	46.3	65.2	93.8
	Changji	99.3	0.3	0.4	83.3	72.2	77.9	86.4	95.9
	Wujiaqu	99.9	0.0	0.1	79.3	72.9	82.3	78.1	84.1
	Urumqi	86.7	13.3	0.0	92.6	92.0	84.6	93.4	100.0
	Fukang	99.6	0.4	0.1	67.0	58.1	38.8	73.7	93.4
Southern slope	Kashi	100.0	0.0	0.0	97.1	98.3	93.0	97.6	99.0
	Artux	100.0	0.0	0.0	88.0	88.1	74.6	89.6	98.4
	Aksu	100.0	0.0	0.0	96.8	97.9	92.6	96.3	100.0
	Korla	100.0	0.0	0.0	87.4	93.7	70.7	89.0	94.4
	Turpan	100.0	0.0	0.0	93.6	96.3	84.2	92.9	99.2
	Hami	100.0	0.0	0.0	88.7	86.6	77.5	94.2	95.5

The nonparametric Sen's slope (Sen 1968) was used to calculate the linear trends during the period 2007–2013, and a trend is considered to be statistically significant if it is significant at the 0.05 level using a Mann-Kendall test (Kendall 1955). For correlation assessments, Pearson's correlation coefficient and two-tailed t test were used.

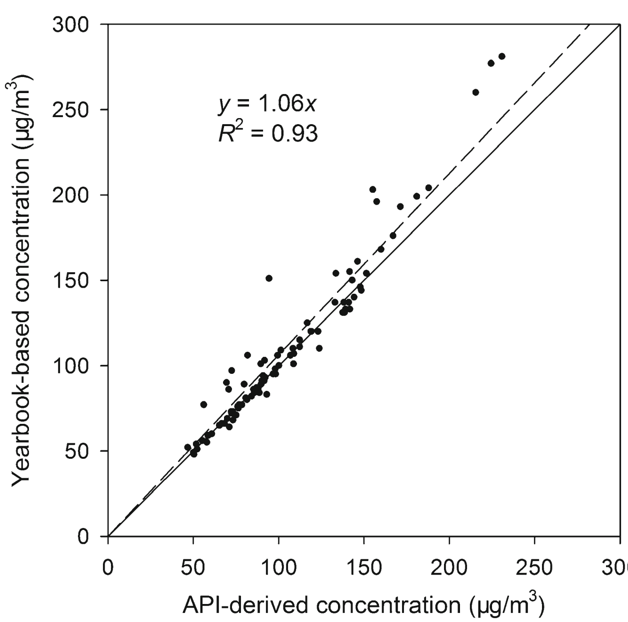

Fig. 2 Scatter plot of the yearbook-based and the API-derived annual mean PM_{10} concentrations for each city around the eastern Tien Shan during 2007–2012. The line of equality is shown as a *solid line*. The yearbook-based annual mean PM_{10} concentrations are acquired from Statistics Bureau of Xinjiang Uygur Autonomous Region (2008, 2009, 2010, 2011, 2012, 2013)

Results

Spatial distribution

Figure 3 shows the spatial distribution of urban PM_{10} concentrations around the eastern Tien Shan. The annual PM_{10} concentrations (±standard deviations) for each city range from 55±28 μg/m^3 in Bole to 195±144 μg/m^3 in Kashi. On an annual basis, PM_{10} concentrations on the northern slope range from 55±28 to 92±75 μg/m^3 (except Urumqi, 144±107 μg/m^3), which is generally lower than those on the southern slope (between 96±65 and 195±144 μg/m^3). Detailed information for each city is also listed in Table S2.

In the spring (Fig. 3b), PM_{10} concentrations for each city on the northern slope (except Urumqi, 119±70 μg/m^3) are generally lower than 100 μg/m^3. However, the seasonal mean concentrations on the southern slope are all larger than 100 μg/m^3. The highest spring mean concentrations are in Kashi, Aksu, and Artux, and the spring PM_{10} concentrations on the southern slope are much larger than that in most regions of China (Qu et al. 2010). In the summer (Fig. 3c), the difference of PM_{10} concentrations between the northern and southern slopes is relatively small, and concentrations in all the cities (except Kashi, 121±82 μg/m^3) are less than 100 μg/

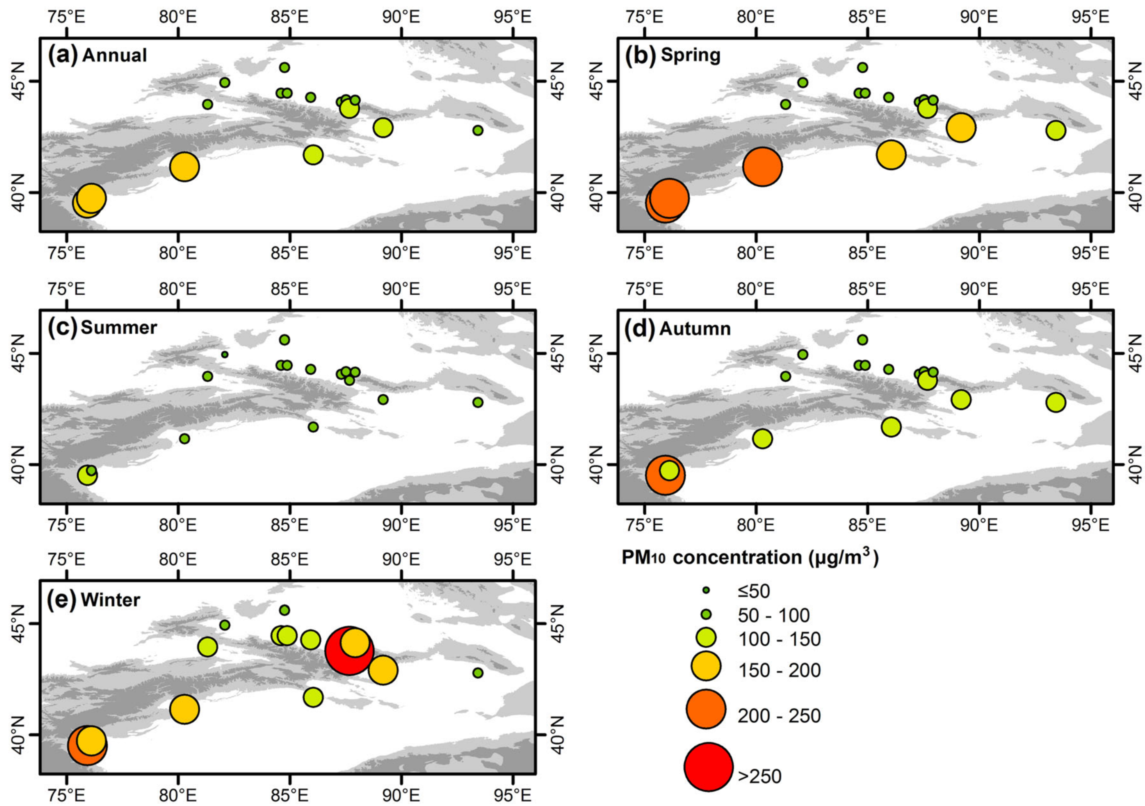

Fig. 3 Spatial distribution of **a** annual and **b**–**e** seasonal urban PM_{10} concentration for each city around the eastern Tien Shan during 2007–2013

m^3. In autumn (Fig. 3d), the spatial distribution is generally similar as that in spring, but the values on the southern slope are less than those in the spring. In the winter (Fig. 3e), PM_{10} concentrations on the southern slope are generally larger than those on the northern slope, but Urumqi on the northern slope shows the maximum value (285±122 μg/m^3).

Seasonal variation

Figure 4a shows the changes in daily urban PM_{10} concentrations for each city over the eastern Tien Shan during the period 2007–2013, and seasonal variations can be seen for the study region. As shown in Fig. 4b, c, the seasonality of PM_{10} concentrations also exists for both the northern and southern slopes, but the peak period is not exactly the same for these two groups. For the northern slope, the high concentration usually occurs between December and February (Fig. 4b). However, the highest PM_{10} concentrations exist between March and April on the southern slope (Fig. 4c). The differences throughout the year are larger on the southern slope than on the northern slope.

More information about PM_{10} concentration extremes for each city is also provided in Fig. S1 in the supplementary material, and here, we focus on the seasonal variation of concentrations on the southern slope. In the spring, the 90th percentiles of PM_{10} concentrations are larger than 300 μg/m^3 (except for Hami). In Kashi, Artux, and Aksu, the 90th percentiles during the spring are higher than 500 μg/m^3. In the summer, the 90th percentiles for each city are generally less than 200 μg/m^3, and the proportions of days with concentration larger than 400 μg/m^3 are all less than 2 % among these cities. In autumn, the 90th percentiles for each city are higher than those during summertime. In the winter, the 90th percentiles are generally similar as those in autumn, but less than those in the spring.

Interannual variation

Figure 5 shows the interannual variability of PM_{10} concentration during the period 2007–2013 for the study region. On an annual basis, there is a nonsignificantly increasing trend for the arithmetic mean concentrations on the northern slope from 2007 to 2013 (0.5 μg/m^3 per year, $p>0.1$). The median (and arithmetic mean) concentrations of annual PM_{10} over the cities on the northern slope range between 60 μg/m^3 (and 72 μg/m^3) in 2010 and 74 μg/m^3 (and 90 μg/m^3) in 2013. On the southern slope, the trend of annual arithmetic mean concentration (9.5 μg/m^3 per year) is also not statistically significant at the 0.05 level. The median (and arithmetic mean) concentrations on the southern slope range between 92 μg/m^3 (and 116 μg/m^3) in 2008 and 144 μg/m^3 (and 192 μg/m^3) in 2013. The annual PM_{10} concentration in 2013 has the highest median and arithmetic mean among the 7 years.

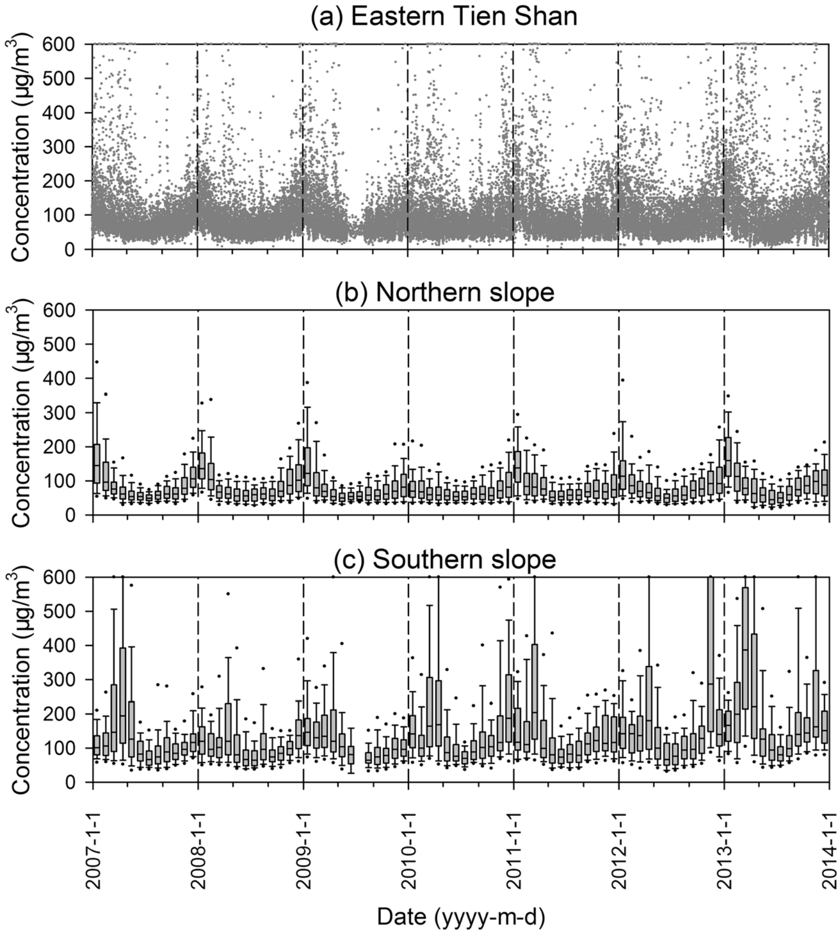

Fig. 4 Variation of daily urban PM_{10} concentration (**a**) and monthly box plots showing daily urban PM_{10} concentration on the northern (**b**) and southern (**c**) slopes for each city around the eastern Tien Shan during 2007–2013. For the box plot on a monthly basis, the *bottom of the box* indicates the 25th percentile, a *line within the box* marks the 50th percentile (median), and the *top of the box* indicates the 75th percentile; *whiskers* indicate the 90th and 10th percentiles; *points above and below the whiskers* show the 95th and 5th percentiles

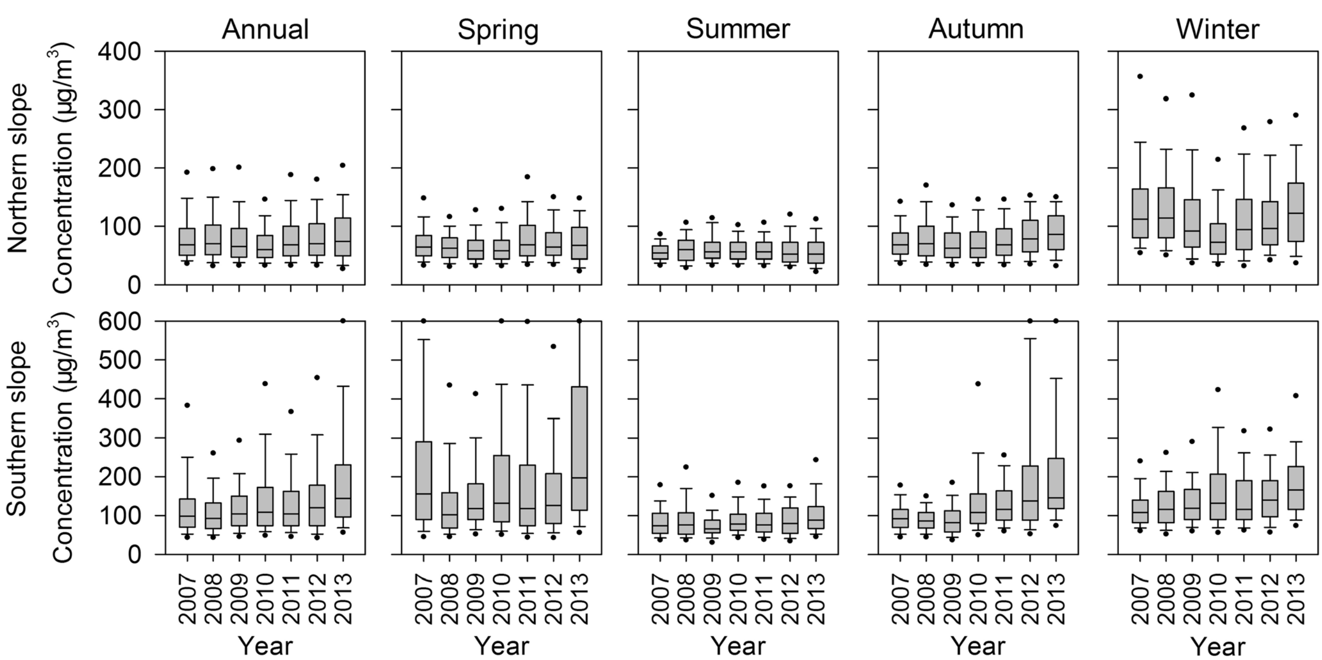

Fig. 5 Interannual variation of urban PM_{10} concentration over the northern (*top*) and southern (*bottom*) slope during 2007–2013. The *bottom of the box* indicates the 25th percentile, a *line within the box* marks the 50th percentile (median), and the *top of the box* indicates the 75th percentile; *whiskers* indicate the 90th and 10th percentiles; *points above and below the whiskers* show the 95th and 5th percentiles

On a seasonal basis, there is no statistically significant trend of arithmetic mean concentration for the cities on the northern slope, and the calculated trend magnitudes are approximately 0.8, −0.3, 2.3, and −2.1 μg/m^3 per year for the spring, summer, autumn, and winter, respectively. PM_{10} concentrations on the southern slope show greater fluctuation, but only the increasing trend in the winter (6.6 μg/m^3 per year) is significant at the 0.05 level. The linear trend magnitudes are 8.7, 2.5, and 20.1 μg/m^3 per year for the spring, summer, and autumn, respectively.

Discussions

PM_{10} concentration and anthropogenic emissions

Anthropogenic emission is usually considered as an important source of atmospheric PM_{10}, especially for the urban environment (e.g., Querol et al. 2001; Artíñano et al. 2003; Rodriguez et al. 2004; Minguillón et al. 2007, 2012; Aldabe et al. 2011; Revuelta et al. 2014). Figure 6a shows the urban population for each city and county near the eastern Tien Shan. Figure 6b, c shows the anthropogenic PM_{10} emissions derived from the Intercontinental Chemical Transport Experiment—Phase B Project (INTEX-B; available at http://mic.greenresource.cn/intex-b2006) and the Regional Emission inventory in Asia (REAS; available at http://www.nies.go.jp/REAS), respectively. The emissions are estimated for all major anthropogenic sources, and calculation process and uncertainties of PM_{10} in these datasets are detailed in Zhang et al. (2009) and Kurokawa et al. (2013). The high PM_{10} emissions usually coincide with the densely populated cities. Such is the case for the city of Urumqi (red spot in Fig. 6a), which is the capital of Xinjiang Uygur Autonomous Region, with a long history of industry and agriculture, and the highest population density in the eastern Tien Shan. PM_{10} emission near Urumqi is the largest of the whole area, with 2×10^4 t/year/grid (a grid is defined as $0.5°\times0.5°$). PM_{10} concentrations in Urumqi are the highest of the northern slope (shown in Fig. 3), hence reflecting the impact of PM_{10} emissions. This is in agreement with previous studies, which also found a great

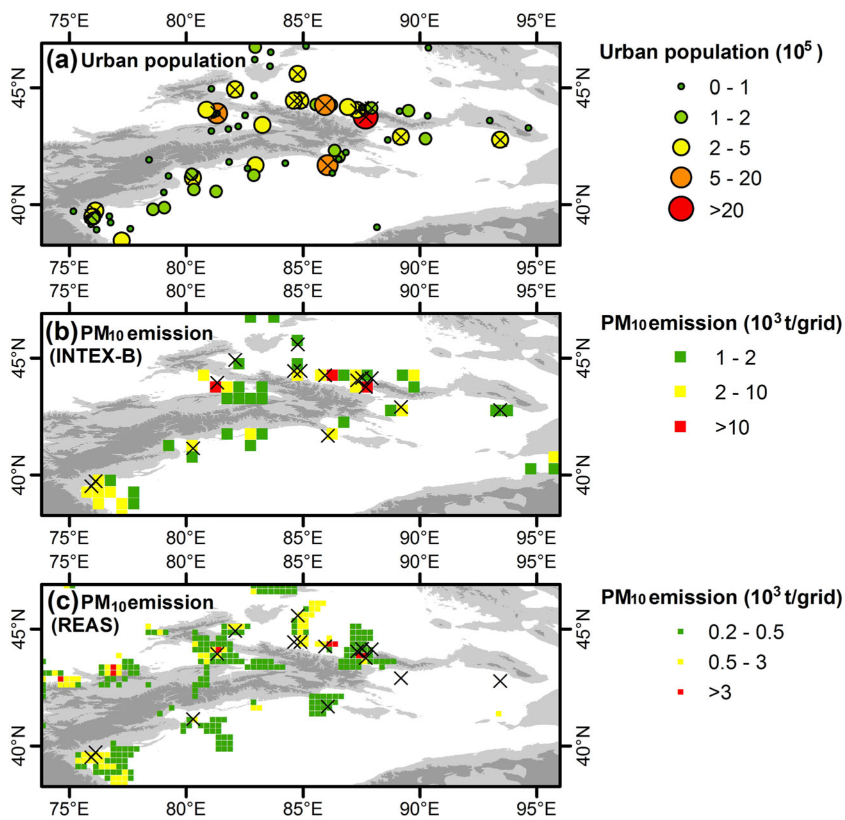

Fig. 6 Spatial distribution of urban population in 2011 (**a**) and anthropogenic PM_{10} emission derived from the Asian Emission Inventory for the Intercontinental Chemical Transport Experiment—Phase B (INTEX-B) mission version 1.2 at $0.5°\times0.5°$ resolution in 2006 (**b**) and from the Regional Emission inventory in Asia (REAS) version 2.1 at $0.25°\times0.25°$ resolution in 2008 (**c**) around the eastern Tien Shan. The urban population in 2011 is acquired from Statistics Bureau of Xinjiang Uygur Autonomous Region (2012). PM_{10} emission sources in INTEX-B mission version 1.2 (Zhang et al. 2009; available at http://mic.greenresource.cn/intex-b2006) and REAS version 2.1 (Kurokawa et al. 2013; available at http://www.nies.go.jp/REAS) mainly include anthropogenic sources such as power plants, industry, transport, and residential and agricultural activities. The sampling sites used in the present study are marked as *black crosses*

impact of human activities in Urumqi's atmospheric aerosol (Li et al. 2008; Mamtimin and Meixner 2011).

Based on the REAS dataset in 2008, the mean emissions of anthropogenic PM_{10} on the northern slope (19.2 t/month/grid) are much larger than those on the southern slope (6.4 t/month/grid). Despite that PM_{10} emissions from most anthropogenic sources (including power and heat plants, industry, road traffic, plane emissions, shipping emissions, etc.) do not have a great seasonal pattern, the emissions generated by domestic heating are clearly higher during the winter (Fig. 7a). The emissions from domestic sources in the winter (6.4 and 2.9 t/month/grid, for northern and southern slopes, respectively) are slightly larger than those in the summer (2.9 and 1.3 t/month/grid). On the northern (and southern) slope, 15 % (and 20.4 %) and 33.2 % (and 43.1 %) of anthropogenic PM_{10} are from domestic sources in the summer and winter, respectively. During winter months, the observed surface air temperature in the study region is much less than ice point (Wang et al. 2014), and domestic heating with coal and natural gas may contribute a lot to the high PM_{10} loading. In addition, the concentration extremes on the northern slope are much larger than those on the southern slope. During winter months, the 95th percentile of monthly PM_{10} emission is larger than 17 t/month/grid on the northern slope, and that is approximately 9 t/month/grid on the southern slope. The great difference between the northern and southern slope can also be seen for the summer months.

Figure 7b shows the increasing trend of soot emissions attributed to the rapid economic development and urbanization of the city belts around the eastern Tien Shan. During the period 2007–2013, the civilian vehicles (including private vehicles) have increased from 818×10^3 to 2433×10^3, which may also influence the interannual variation of PM_{10} concentrations. However, in this study, the PM_{10} concentration did not change significantly from 2007 to 2013, and the increasing investment in antipollution projects by local government during the recent decade cannot be ignored.

The PM_{10} emissions near Urumqi, Shihezi, and Yining on the northern slope of the eastern Tien Shan are higher than 10^4 t/year/grid (a grid is defined as $0.5°\times0.5°$) (Fig. 6b), and these cities are the largest three cities in the population list (see Table S1 in the supplementary material) on the northern slope. But, the PM_{10} concentrations on the northern slope are generally lower than those on the southern slope. Hence, there are additional factors driving the PM_{10} concentrations in the Tien Shan, such as dust events and precipitation, which will be discussed in later sections.

PM_{10} concentration and Asian dust source

In the past decades, many studies have demonstrated the impact of dust events on atmospheric PM_{10} (Rodriguez et al. 2001; Pey et al. 2013; Krasnov et al. 2014; Dimitriou and Kassomenos 2013, 2014). The central Asia is commonly known as a dust source at global and regional scale, and it can reach other areas by long-range transport (Liu et al. 2009; Ku and Park 2013). Previous investigations also showed that dust concentration in ice core and glacier snowpack acquired from this region is generally higher than that acquired from the polar regions and European Alps (Dong et al. 2009, 2010; Wu et al. 2010). Dust events were more frequent on the southern slope (Fig. S2 in the supplementary material) during 1981–2010, and the largest frequency of dust events

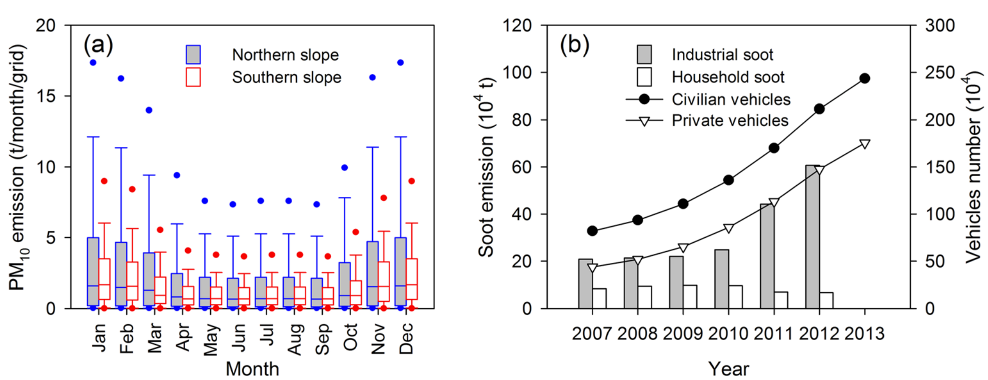

Fig. 7 **a** Monthly distribution of PM_{10} emission from domestic sources in 2008 derived from the Regional Emission Inventory in Asia (REAS) version 2.1 at $0.25°\times0.25°$ resolution. The northern slope is defined as the region between 75° E and 95° E (longitude) and between 43° E and 45° E (latitude), and the southern slope is between 75° E and 95° E (longitude) and between 40° E and 43° E (latitude). The data are available at http://www.nies.go.jp/REAS, and the details are described in Kurokawa et al. (2013). The *bottom of the box* indicates the 25th percentile, a *line within the box* marks the 50th percentile (median), and the *top of the box* indicates the 75th percentile; *whiskers* indicate the 90th and 10th percentiles; *points above and below the whiskers* show the 95th and 5th percentiles. **b** Changes in annual soot emission and registered civilian vehicles in Xinjiang during 2007–2013 (Statistics Bureau of Xinjiang Uygur Autonomous Region 2008, 2009, 2010, 2011, 2012, 2013; Statistics Bureau of Xinjiang Uygur Autonomous Region and State Statistics Bureau 2014). Soot emission mainly includes industrial and household soot, and registered civilian vehicles can be classified into private and non-private vehicles

takes place in the spring. So, in this section, we focus on the relationship between PM_{10} concentration and dust events during springtime.

Figure 8 demonstrates the correlation between spring PM_{10} concentration and the proportion of dust event days for each sampling site on a seasonal basis. Good correlations (R^2= 0.383, p<0.001) and positive slopes can be seen for the southern slope, but there is no significant correlation (R^2=0.001, p>0.1) for the northern slope. The high PM_{10} loadings widely occur during the spring especially for the cities on the southern slope, so the influence of dust events on PM_{10} concentration is critical for the spatial distribution during the spring. As shown in Table 3, PM_{10} concentrations in dust event days are generally higher than those in nondust days, and the concentration difference is even up to 334 μg/m^3 for the Turpan station on the southern slope. It must be also that the proportion of dust days on the northern slope is much lower than that on the southern slope, and the concentration difference between the two conditions is relatively small on the northern slope.

To investigate the air mass origin reaching the study areas, 3-day back-trajectories during springtime were calculated daily for two different altitudes (500 and 1500 m above ground level) with the HYSPLIT model (Draxler and Hess 1998). Each backward trajectory for two representative cities in the middle section of the eastern Tien Shan (Changji on the northern slope, and Korla on the southern slope) is shown in

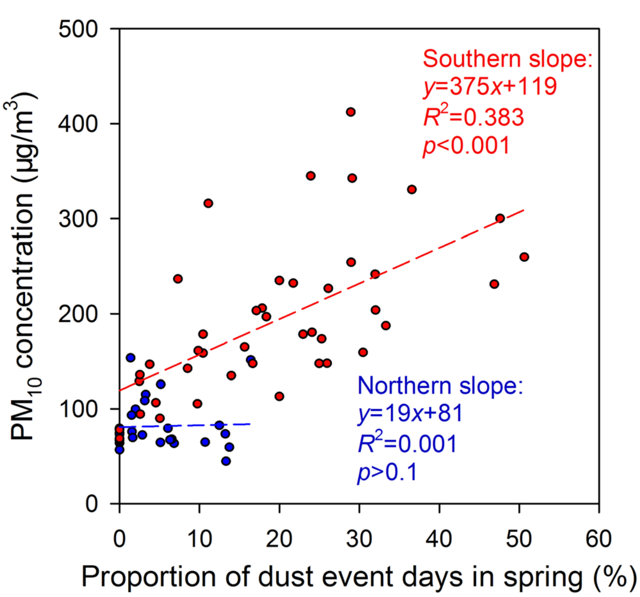

Fig. 8 Scatter plot of PM_{10} concentration in the spring versus the proportion of dust event days for each spring and each city around the eastern Tien Shan during 2007–2013. Northern slope (*blue color*), Yining, Usu, Karamay, and Urumqi; southern slope (*red color*), Kashi, Artux, Aksu, Korla, Turpan, and Hami. Precipitation days (daily precipitation >0 mm) are excluded

Fig. 9 and colored depending on the daily PM_{10} concentration measured on the ending day. Although the distance between the two cities is less than 300 km, the PM_{10} concentrations on the southern slope are higher than those on the northern slope. The trajectories from the northwestern direction usually have low particulate matter loading, but those passing the great dust source Taklimakan Desert (south of the Tien Shan) have very high PM_{10} concentration. On the southern slope, the contribution of "clean" air from the northwestern direction is limited, and the trajectories crossing the southern desert play a dominant role. The specific geography of the area hinders the dust aerosol from the southern desert to reach the northern slope, probably because the local dust transport takes place at lower height than the mountain height. The long-range dust transport usually takes place at high altitudes, but the orography of the area allows us to estimate that the dust may travel lower than approximately 3000 m above ground level (a.g.l.). The Asian dust source (especially Taklimakan Desert) has great influence on the urban PM_{10} concentration on the southern slope, and the impact is relatively weak on the northern slope.

PM_{10} concentration and atmospheric condition

The height of the boundary layer (mixing layer height) is related with the thermal inversions in atmosphere, which is an important factor controlling urban air quality (Mamtimin and Meixner 2011). Figure 10a shows the seasonal changes in the boundary layer depth in Urumqi in 2013. The boundary layer height was calculated using the global NCEP GDAS archive data (1°×1°, three hourly). The height in the winter is significantly lower (<200 m) than that in the summer (>600 m). The obvious seasonality of boundary layer height in Fig. 10a indicates that the winter usually suffers near-surface thermal inversions, which may significantly hinder the transportation of particulate matter loadings. The seasonality can also be detected in other cities around the Tien Shan, and the winter meteorological condition in the area is not propitious to the dispersion of urban particulate matter loading. The atmospheric stability can be classified into seven levels according to the Pasquill stability class (Pasquill 1961). As shown in Fig. 10b, the atmosphere conditions in the winter are generally stable, and the proportion of unstable conditions in the summer is greatly larger than that in the winter. The stable condition is usually featured as low solar radiation and/or wind speed, and the particulate matter may be relatively stable at a high concentration.

In addition, ambient particulate matter can be removed by a scavenging effect of precipitation. The difference of PM_{10} concentration (Δc) between pre-precipitation day (the rainless day before precipitation day) and precipitation day is

Table 3 Average spring PM_{10} concentration during nondust and dust event days, difference of PM_{10} concentration (Δc) in μg/m^3 and in percent with respect to the concentration in nondust event days, and proportion of dust event days in the spring for each city around the eastern Tien Shan during 2007–2013

City		PM_{10} concentration (μg/m^3)		Δc		Proportion of dust days (%)
		Non-dust days	Dust days	μg/m^3	%	
Northern slope	Yining	78	73	−5	−6	2
	Usu	67	90	23	34	3
	Karamay	62	69	8	12	10
	Urumqi	125	176	51	41	6
Southern slope	Kashi	200	361	161	81	33
	Artux	181	363	182	100	24
	Aksu	178	359	180	101	29
	Korla	131	349	218	166	21
	Turpan	136	470	334	245	10
	Hami	102	280	178	176	2

Bole, Kuytun, Shihezi, Changji, Wujiaqu, and Fukang are not calculated due to missing data. Precipitation days are excluded

presented in Table 4. As the pre-precipitation PM_{10} concentration increases, Δc is more and more apart from 0, and the change rates of daily concentration decrease from 5.4 % (all events) to 31.1 % (pre-precipitation PM_{10} concentration >300 μg/m^3). The rainfall or snowfall during dirty days has great effect in reducing PM_{10} loadings, and the effect is usually greater in heavier precipitation events. For the daily PM_{10} concentration larger than 200 μg/m^3, daily precipitation time for dust events in the study region (Wang et al. 2003). The Tien Shan (mountain ridge) and Taklimakan Desert on the southern Tien Shan is marked as *black curves* and *dotted area*, respectively. Satellite-derived land cover and shaded relief are acquired from Natural Earth (http://www.naturalearthdata.com)

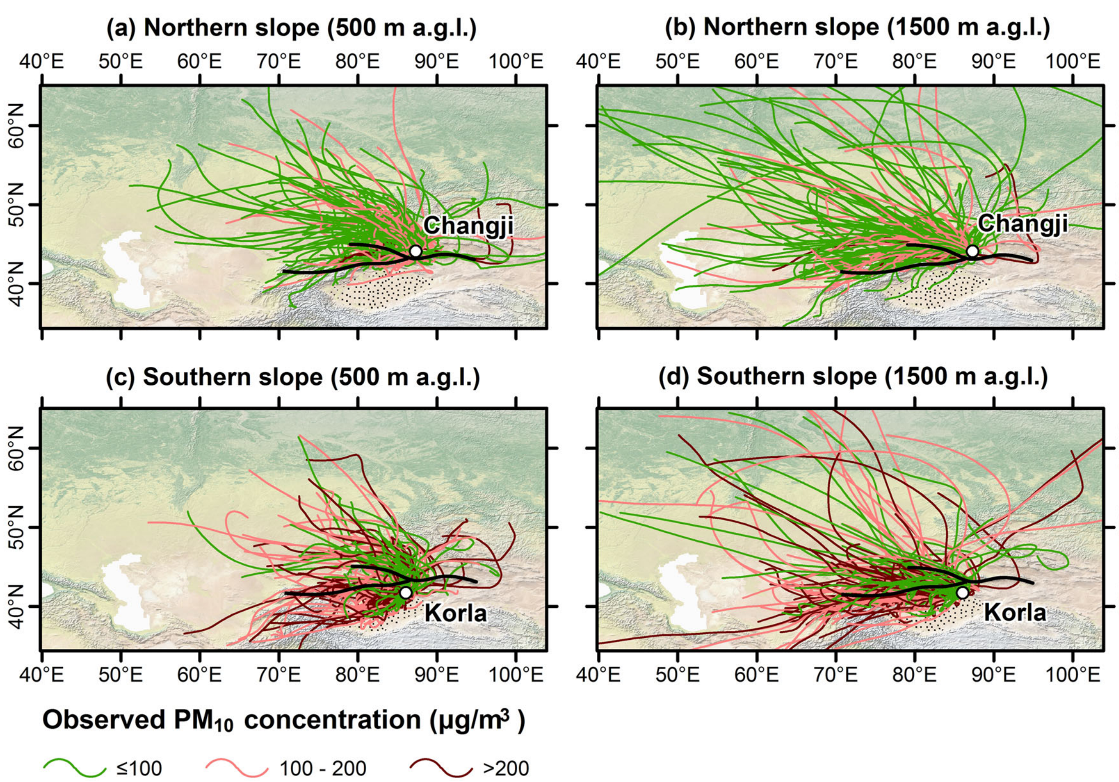

Fig. 9 3-day back-trajectories for (**a**, **b**) Changji, on the northern slope, and (**c**, **d**) Korla, on the southern slope, for two different heights (500 and 1500 m above ground level) for each day during spring 2007–2013 using the HYSPLIT model and NCEP/NCAR Reanalysis. Each trajectory is colored depending on the daily PM_{10} concentration measured on the last day. The starting time is set at 18:00 Beijing Time (16:00 LST), a peak

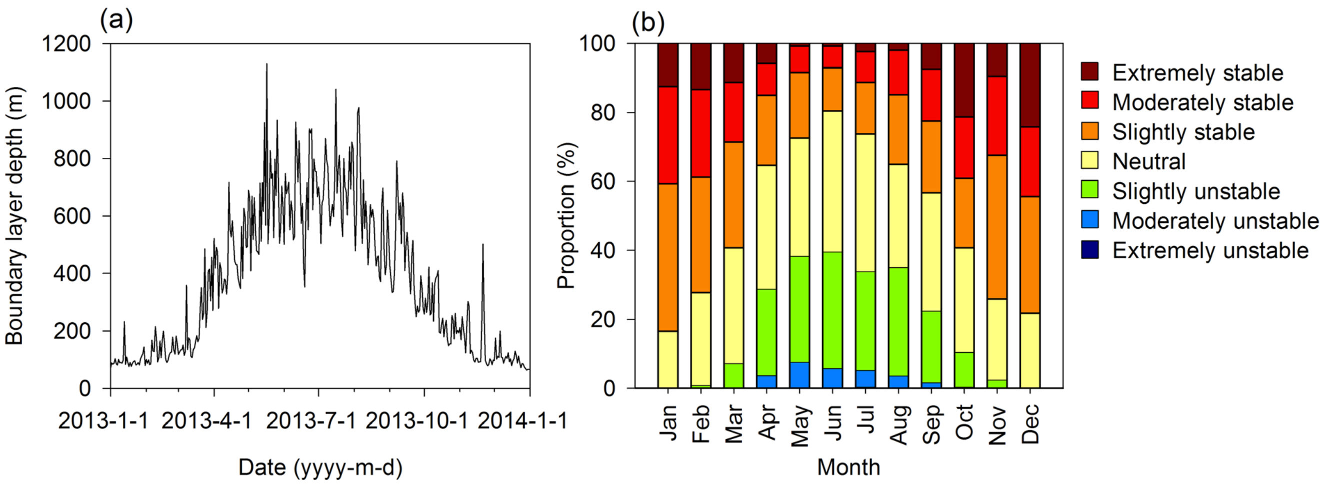

Fig. 10 Variation of **a** daily mean boundary layer depth and **b** monthly Pasquill stability class in Urumqi during 2013. The data are calculated using NOAA's Real-time Environmental Applications and Display System (READY) and NCEP Global Data Assimilation System (GDAS) archive data (1°×1°, three hourly). The atmospheric stability is expressed using the Pasquill stability class (Pasquill 1961)

≥10 mm may remove 43.4 % of the PM_{10} loading, while the PM_{10} reduction is 5.4 % for all the precipitation events and all the initial concentrations.

According to the long-term climatology during 1981–2010 (see Fig. S3 in the supplementary material), precipitation on the northern slope is significantly larger than that on the southern slope, which is mainly impacted by the moisture from westerlies and polar air mass (Tian et al. 2007). The most abundant rainfall occurs in the summer, which may cause great scavenging of PM_{10} during this season.

Concluding remarks

In this paper, the daily urban PM_{10} concentration in 16 cities around the eastern Tien Shan during 2007–2013 was assessed, and related anthropogenic and natural factors influencing the PM_{10} distribution were discussed. Compared with the northern slope of the eastern Tien Shan, cities on the southern slope generally have higher PM_{10} concentration on an annual basis. For the northern slope, the winter is the season with the highest PM_{10} concentration, whereas this happens in the spring on the southern slope. The northern slope usually has heavy anthropogenic air pollution (mostly in the winter) and rich precipitation especially in the summer, with the resulting scavenging and decrease of ambient PM_{10} concentrations, but the southern slope is affected frequently by dust events (mostly in the spring) and less precipitation. Asian dust source is an important factor causing the high particulate matter loading during springtime. Taklimakan Desert near the Tien Shan is considered to be a vital dust aerosol source influencing the study area. Modeled back-trajectory indicated that the southern desert source can greatly increase the PM_{10} concentration on the southern slope, and the Tien Shan may hinder the dust transport to the northern slope.

Table 4 Difference of PM_{10} concentration (Δc) in μg/m³ and in percent with respect to the highest concentration between precipitation day and pre-precipitation at different conditions over the eastern Tien Shan from January 2007 to September 2013

Pre-precipitation concentration (μg/m³)	Precipitation >0 mm			Precipitation ≥1 mm			Precipitation≥10 mm		
	Δc		*N*	Δc		*N*	Δc		*N*
	(μg/m³)	(%)		(μg/m³)	(%)		(μg/m³)	(%)	
>0	5.2	5.4	2,068	6.8	7.4	1,019	4.2	4.9	97
>100	28.1	16.4	614	30.3	18.2	282	37.6	25.8	25
>200	72.7	22.7	132	84.9	24.8	48	100.7	43.4	3
>300	134.2	31.1	57	136.9	29.7	23			

N is number of records. Kuytun, Changji, Wujiaqu, and Fukang during 2007–2013; Bole and Artux during 2007–2008; and Shihezi during 2009–2013 are not calculated due to missing data of daily precipitation

Acknowledgments This research was supported by the National Basic Research Program of China (973 Program) (No. 2013CBA01801) and the National Natural Science Foundation of China (No. 41161012 and 41201065). We are very grateful to an anonymous reviewer for the constructive suggestions.

References

Aldabe J, Elustondo D, Santamaría C, Lasheras E, Pandolfi M, Alastuey A, Querol X, Santamaría JM (2011) Chemical characterisation and source apportionment of $PM_{2.5}$ and PM_{10} at rural, urban and traffic sites in Navarra (North of Spain). Atmos Res 102:191–205

Artíñano B, Salvador P, Alonso DG, Querol X, Alastuey A (2003) Anthropogenic and natural influence on the PM_{10} and $PM_{2.5}$ aerosol in Madrid (Spain): analysis of high concentration episodes. Environ Pollut 125:453–465

Chen BB, Sverdlik LG, Imashev SA, Solomon PA, Lantz J, Schauer JJ, Shafer MM, Artamonova MS, Carmichael G (2013) Empirical relationship between particulate matter and aerosol optical depth over Northern Tien-Shan, Central Asia. Air Qual Atmos Health 6: 385–396

Choi Y-S, Ho C-H, Chen D, Noha Y-H, Song C-K (2008) Spectral analysis of weekly variation in PM10 mass concentration and meteorological conditions over China. Atmos Environ 42:655–666

Dimitriou K, Kassomenos P (2013) The fine and coarse particulate matter at four major Mediterranean cities: local and regional sources. Theor Appl Climatol 114:375–391

Dimitriou K, Kassomenos P (2014) Decomposing the profile of PM in two low polluted German cities–mapping of air mass residence time, focusing on potential long range transport impacts. Environ Pollut 190:91–100

Dong Z, Li Z, Wang F, Zhang M (2009) Characteristics of atmospheric dust deposition in snow on the glaciers of the eastern Tien Shan, China. J Glaciol 55:797–804

Dong Z, Li Z, Xiao C, Wang F, Zhang M (2010) Characteristics of aerosol dust in fresh snow in the Asian dust and non-dust periods at Urumqi glacier no. 1 of eastern Tian Shan, China. Environ Earth Sci 60: 1361–1368

Dong Z, Qin D, Kang S, Ren J, Chen J, Cui X, Du Z, Qin X (2014) Physicochemical characteristics and sources of atmospheric dust deposition in snow packs on the glaciers of western Qilian Mountains, China. Tellus B 66. doi:10.3402/tellusb.v66.20956

Draxler RR, Hess GD (1998) An overview of the HYSPLIT_4 modeling system of trajectories, dispersion, and deposition. Aust Meteorol Mag 47:295–308

Feng Y, Peng L, Wu J, Zhu T, Lv A, Zhang K (2005) Analytic studies on source of TSP and PM_{10} in environmental air of Urumchi city. China Environ Sci 25:30–33

Gong D-Y, Ho C-H, Chen D, Qian Y, Choi Y-S, Kim J (2007) Weekly cycle of aerosol-meteorology interaction over China. J Geophys Res 112:D22202. doi:10.1029/2007JD008888

Groll M, Opp C, Aslanov I (2013) Spatial and temporal distribution of the dust deposition in Central Asia – results from a long term monitoring program. Aeolian Res 9:49–62

Gu C, Guo Y (2010) Discussion of quality control road-inspection on PM_{10} auto-monitoring instrument for city environmental air in Xinjiang. Arid Environ Monitor 24:34–38

Guo Y, Wang Z, Kang H, Zhang X, Ji Y, Li J, Chen H (2014) Influence of monitoring index TSP and PM_{10} on ambient air quality grade at cities of Xinjiang, China. Arid Land Geog 37:731–743

Han X, Wei W, Liu M, Hong W, Lu H, Zhang Y (2013) The influences of airflow on the concentrations of PM_{10}, $PM_{2.5}$ and $PM_{1.0}$ in Urumqi, Xinjiang, China. J Desert Res 33:223–230

Han Y, Fang X, Kang S, Wang H, Kang F (2008) Shifts of dust source regions over central Asia and the Tibetan Plateau: connections with the Arctic oscillation and the westerly jet. Atmos Environ 42:2358–2368

Kendall MR (1955) Rank correlation methods. Charles Griffin, London

Krasnov H, Katra I, Koutrakis P, Friger MD (2014) Contribution of dust storms to PM_{10} levels in an urban arid environment. J Air Waste Manag Assoc 64:89–94

Ku B, Park RJ (2013) Comparative inverse analysis of satellite (MODIS) and ground (PM_{10}) observations to estimate dust emissions in East Asia. Asia Pac J Atmos Sci 49:3–17

Kurokawa J, Ohara T, Morikawa T, Hanayama S, Janssens-Maenhout G, Fukui T, Kawashima K, Akimoto H (2013) Emissions of air pollutants and greenhouse gases over Asian regions during 2000–2008: Regional Emission inventory in ASia (REAS) version 2. Atmos Chem Phys 13:11019–11058

Li J, Xiong A (2004) Summary of research on meteorological scientific data sharing system. J Appl Meteorol Sci 15:1–9

Li J, Zhuang G, Huang K, Lin Y, Xu C, Yu S (2008) Characteristics and sources of air-borne particulate in Urumqi, China, the upstream area of Asia dust. Atmos Environ 42:776–787

Li Z, Zhao S, Edwards R, Wang W, Zhou P (2011) Characteristics of individual aerosol particles over Ürümqi Glacier No. 1 in eastern Tianshan, central Asia, China. Atmos Res 99:57–66

Liu T-H, Tsai F, Hsu S-C, Hsu C-W, Shiu C-J, Chen W-N, Tu J-Y (2009) Southeastward transport of Asian dust: source, transport and its contributions to Taiwan. Atmos Environ 43:458–467

Ma L, Cao L, Li Y, Liu X (2010) Monitoring and analysis of PM_{10} at different districts of Urumqi City. Arid Land Geog 33:231–235

Maher BA, Prospero JM, Mackie D, Gaiero D, Hesse PP, Balkanski Y (2010) Global connections between aeolian dust, climate and ocean biogeochemistry at the present day and at the last glacial maximum. Earth-Sci Rev 99:61–97

Mamtimin B, Meixner FX (2011) Air pollution and meteorological processes in the growing dryland city of Urumqi (Xinjiang, China). Sci Total Environ 409:1277–1290

Minguillón MC, Querol X, Alastuey A, Monfort E, Miró VJ (2007) PM sources in a highly industrialised area in the process of implementing PM abatement technology: quantification and evolution. J Environ Monitor 9:1071–1081

Minguillón MC, Querol X, Baltensperger U, Prévôt ASH (2012) Fine and coarse PM composition and sources in rural and urban sites in Switzerland: local or regional pollution? Sci Total Environ 427–428:191–202

Ministry of Environmental Protection of China (2011) Environmental protection industry standard of the People's Republic of China: determination of atmospheric articles PM_{10} and $PM_{2.5}$ in ambient air by gravimetric method (HJ618-2011). China Environmental Science Press, Beijing

Pasquill F (1961) The estimation of the dispersion of windborne material. Meteorol Mag 90:33–49

Pey J, Querol X, Alastuey A, Forastiere F, Stafoggia M (2013) African dust outbreaks over the Mediterranean Basin during 2001–2011: PM10 concentrations, phenomenology and trends, and its relation with synoptic and mesoscale meteorology. Atmos Chem Phys 13: 1395–1410

Qu WJ, Arimoto R, Zhang XY, Zhao CH, Wang YQ, Sheng LF, Fu G (2010) Spatial distribution and interannual variation of surface PM_{10} concentrations over eighty-six Chinese cities. Atmos Chem Phys 10: 5641–5662

Querol X, Alastuey A, Rodriguez S, Plana F, Mantilla E, Ruiz CR (2001) Monitoring of PM10 and PM2.5 around primary particulate anthropogenic emission sources. Atmos Environ 35:845–858

Revuelta MA, McIntosh G, Pey J, Pérez N, Querol X, Alastuey A (2014) Partitioning of magnetic particles in PM_{10}, $PM_{2.5}$ and PM_1 aerosols in the urban atmosphere of Barcelona (Spain). Environ Pollut 188: 109–117

Rodriguez S, Querol X, Alastuey A, Kallos G, Kakaliagou O (2001) Saharan dust contributions to PM10 and TSP levels in Southern and Eastern Spain. Atmos Environ 35:2433–2447

Rodriguez S, Querol X, Alastuey A, Viana M-M, Alarcón M, Mantilla E, Ruiz CR (2004) Comparative PM10-PM2.5 source contribution study at rural, urban and industrial sites during PM episodes in Eastern Spain. Sci Total Environ 328:95–113

Sen PK (1968) Estimates of the regression coefficient based on Kendall's tau. J Am Stat Assoc 63:1379–1389

State Environmental Protection Administration of China (2003) Environmental protection industry standard of the People's Republic of China: specifications and test procedures for PM_{10} sampler (HJ/T 93–2003). China Environmental Science Press, Beijing

Statistics Bureau of Xinjiang Uygur Autonomous Region (2008) Xinjiang statistical yearbook 2008. China Statistics Press, Beijing

Statistics Bureau of Xinjiang Uygur Autonomous Region (2009) Xinjiang statistical yearbook 2009. China Statistics Press, Beijing

Statistics Bureau of Xinjiang Uygur Autonomous Region (2010) Xinjiang statistical yearbook 2010. China Statistics Press, Beijing

Statistics Bureau of Xinjiang Uygur Autonomous Region (2011) Xinjiang statistical yearbook 2011. China Statistics Press, Beijing

Statistics Bureau of Xinjiang Uygur Autonomous Region (2012) Xinjiang statistical yearbook 2012. China Statistics Press, Beijing

Statistics Bureau of Xinjiang Uygur Autonomous Region (2013) Xinjiang statistical yearbook 2013. China Statistics Press, Beijing

Statistics Bureau of Xinjiang Uygur Autonomous Region, Xinjiang Investigation Team of State Statistics Bureau (2014) Statistical Communiqué on the National Economy and Social Development of Xinjiang Uygur Autonomous Region in 2013. Accessed 27 February 2014

Tian L, Yao T, Macclune K, White JWC, Schilla A, Vaughn B, Vachon R, Ichiyanagi K (2007) Stable isotopic variations in west China: a consideration of moisture sources. J Geophys Res 112: D10112. doi:10.1029/2006JD007718

Wang B (2004) A study on synthetic differentiation method for basic meteorological data quality control. J Appl Meteorol Sci 15:51–59

Wang S, Wang J, Zhou Z, Shang K (2005a) Regional characteristics of three kinds of dust storm events in China. Atmos Environ 39:509–520

Wang S, Zhang M, Sun M, Wang B, Huang X, Wang Q, Feng F (2014) Comparison of surface air temperature derived from NCEP/DOE R2, ERA-Interim, and observations in the arid northwestern China: a consideration of altitude errors. Theor Appl Climatol. doi:10.1007/s00704-014-1107-1

Wang X, Ma Y, Chen H (2003) Climatic characteristics of sandstorm in Xinjiang. J Desert Res 23:539–544

Wang Y, Stein AF, Draxler RR, de la Rosa JD, Zhang X (2011) Global sand and dust storms in 2008: observation and HYSPLIT model verification. Atmos Environ 45:6368–6381

Wang Y, Wang J, Qi Y, Yan C (2005b) Dataset of desert distribution in China (1: 100,000). Environmental and Ecological Science Data Center for West China, National Natural Science Foundation of China, China. doi:10.3972/westdc.006.2013.db

Wang YQ, Zhang XY, Gong SL, Zhou CH, Hu XQ, Liu HL, Niu T, Yang YQ (2008) Surface observation of sand and dust storm in East Asia and its application in CUACE/Dust. Atmos Chem Phys 8:545–553

Wei J (2012) Air pollution and spatial variation of pollutes in Urumqi. J Arid Land Resour Environ 26:67–70

Wei Y (2011) Analysis on variation trend of atmospheric environmental quality in Urumqi. J Environ Prot Sci 37:4–7

Wu G, Zhang X, Zhang C, Gao S, Li Z, Wang F, Wang W (2010) Concentration and composition of dust particles in surface snow at Urumqi Glacier No. 1, Eastern Tien Shan. Global Planet Chang 74: 34–42

Yabuki S, Mikami M, Nakamura Y, Kanayama S, Fu FF, Liu MZ, Zhou HF (2005) The characteristics of atmospheric aerosol at Aksu, an Asian dust-source region of North-West China: a summary of observations over the three years from March 2001 to April 2004. J Meteorol Soc Jpn 83A:45–72

Zhang Q, Streets DG, Carmichael GR, He KB, Huo H, Kannari A, Klimont Z, Park IS, Reddy S, Fu JS, Chen D, Duan L, Lei Y, Wang LT, Yao ZL (2009) Asian emissions in 2006 for the NASA INTEX-B mission. Atmos Chem Phys 9:5131–5153

Zhang XY, Gong SL, Shen ZX, Mei FM, Xi XX, Liu LC, Zhou ZJ, Wang D, Wang YQ, Cheng Y (2003) Characterization of soil dust aerosol in China and its transport and distribution during 2001 ACE-Asia: 1. Network observations. J Geophys Res 108. doi:10.1029/2002JD002632

Zhao S, Li Z, Zhou P (2011) Ion chemistry and individual particle analysis of atmospheric aerosols over Mt. Bogda of eastern Tianshan Mountains, Central Asia. Environ Monitor Ass 180:409–426

Zheng J (2014) Fuzzy mathematics based comprehensive evaluation of atmospheric environmental quality of Urumqi from 2001 to 2011. Environ Pollut Control J 36:28–41